HHS Public Access

Author manuscript

J Immunol. Author manuscript; available in PMC 2018 March 01.

Published in final edited form as:

J Immunol. 2017 March 01; 198(5): 2017–2027. doi:10.4049/jimmunol.1600764.

Antigen processing in the ER is monitored by semi-invariant αβ TCRs specific for a conserved peptide-Qa-1^{b} MHC Ib ligand[1]

Jian Guan[2,3], **Soo Jung Yang**[3], **Federico Gonzalez**[3], **Yuxin Yin**[2], and **Nilabh Shastri**[3]

[2]Institute of Systems Biomedicine, Department of Pathology, School of Basic Medical Sciences, Peking University Health Science Center, Beijing 100191, P.R.China

[3]Division of Immunology and Pathogenesis, Department of Molecular and Cell Biology, University of California, Berkeley, CA 94720, USA

Abstract

Antigen processing in the endoplasmic reticulum (ER) by ERAAP, the ER aminopeptidase associated with antigen processing is central to presentation of a normal peptide-MHC class I repertoire. Alternations in ERAAP function cause dramatic changes in the MHC I presented peptides which elicit potent immune responses. An unusual subset of CD8^{+} T cells monitor normal antigen processing by responding to a highly conserved FL9 peptide that is presented by Qa-1^{b}, a non-classical MHC Ib molecule (QFL) in ERAAP-deficient cells. To understand the structural basis for recognition of the conserved ligand, we analyzed the αβ TCRs of QFL-specific T cells. Individual cells in normal wild-type and TCR β transgenic mice were assessed for QFL-specific TCR α-and β-chains. The QFL-specific cells expressed a predominant semi-invariant TCR generated by DNA rearrangement of TRAV9d-3-TRAJ21 alpha and TRBV5-TRBD1-TRBJ2-7 beta chain gene segments. Further, the CDR3 regions of the α as well as β chains were required for QFL ligand recognition. Thus, the αβ TCRs used to recognize the peptide-Qa-1 ligand presented by ERAAP-deficient cells are semi-invariant and likely reflect conserved mechanism for monitoring the fidelity of antigen processing in the ER.

Keywords

αβ TCR; Antigen presentation; non-classical MHC Ib; pMHC ligands

[1]This work was supported by grants from the NIAID and the NIH to N.S. JG was supported by grant from Chinese Scholarship Council.

Correspondence to: Yuxin Yin; Nilabh Shastri.

[4]Correspondence: Nilabh Shastri, Division of Immunology and Pathogenesis, Department of Molecular and Cell Biology, University of California, Berkeley, CA 94720, USA. Tel: +1 510 643 9197; nshastri@berkeley.edu

[4]Address correspondence and reprint requests to N.S.

Author Contribution

JG, FG and SJY conducted the experimental protocols and analyzed data together with NS. NS, JG and YY wrote the manuscript in consultation with other authors.

Conflict of interest

The authors declare they have no conflict of interest

The sequence data has been deposited in GenBank (https://www.ncbi.nlm.nih.gov/genbank/) under accession numbers KY271957 and KY271958.

Introduction

Major histocompatibility complex (MHC) class I molecules present a large repertoire of peptides on cell surface. These peptides are derived from virtually all intracellular proteins as well as those derived from infecting microbes or mutations in cancer cells. Because the peptide-MHC I (pMHC I) complexes serve as ligands for the T cell antigen receptors (TCRs) expressed on cytotoxic $CD8^+$ T lymphocytes (CTLs), the abnormal cells displaying foreign peptides are efficiently detected and eliminated (1–3).

Generation of pMHC I is a function of the antigen processing pathway which involves a series of concerted steps (4, 5). The protein precursors are first fragmented by the proteasome in the cytoplasm and the fragments are transported into the endoplasmic reticulum (ER) by the TAP transporter (6). In the ER, the peptide intermediates are further trimmed to generate the final peptides that are loaded onto MHC I molecules and the pMHC I complex is transported to the cell surface (7, 8). Failure of any of these steps leads to profound immunological consequences (6, 9–13). Thus, it is critical to monitor the antigen processing pathway for abnormal functioning.

ERAAP, the aminopeptidase associated with antigen processing in the ER, is the protease that plays a major role in customizing peptides in the endoplasmic reticulum (ER) where it trims peptide precursors with amino terminal extensions to their final length (7, 8, 14). The critical function of ERAAP in the antigen processing pathway was established by studies that showed that impaired ERAAP function is associated with profound changes in the pMHC I repertoire that in turn elicit potent immune responses (11, 15–17). Furthermore, polymorphic versions of ERAP1, the human ortholog of mouse ERAAP are associated with autoimmune diseases as well as poor prognosis of tumors (11, 18–20). Notably, a unique $CD8^+$ T cell population was discovered to be responsible for monitoring the normal function of ERAAP (21). These T cells recognize the peptide FYAEATPML (FL9) derived from the *Fam49b* gene that is conserved from humans to zebra fish. The conserved FL9 peptide is presented by Qa-1^b, a non-classical MHC class Ib molecule (Qa1-FL9 or QFL) exclusively by ERAAP deficient cells. In addition to their highly conserved ligand specificity, the QFL-specific T cell population is characterized by its relative abundance and antigen-experienced phenotype in naïve mice (21). How the αβ TCRs of QFL-specific T cells recognize their conserved ligand is not known.

T cell responses usually involve recognition of particular pMHC I ligands by diverse TCRs, although examples of biased TCR usage have been described (22). Notably, mouse invariant natural killer T cells (iNKT) specific for the glycolipid α-galactosylceramide (α-GalCer) presented by CD1d, another non-classical MHC Ib molecule express an invariant TCR α-chain paired with a limited number of β-chains (23). Similarly, T cells that recognize vitamin B metabolites presented by MR1, the MHC class I-like molecule - called Mucosal-associated invariant T cells (MAITs) - also bear invariant TCR α-chains paired with a limited array of β-chains (24, 25).

Here we analyzed the α and β subunits of TCRs used by the QFL-specific T cells. We show that like the TCRs of iNKT and MAIT cells specific for non-peptidic materials presented by

MHC Ib molecule, the FL9 peptide Qa-1 MHC Ib specific TCRs are also semi-invariant. However, the QFL-specific T cells share some but not all characteristics with their iNKT and MAIT cell counterparts.

Materials and methods

DNA constructs, transfection and retroviral transduction

The cDNA encoding the V and J regions of the TCR α- and β-chain of BEko8Z hybridoma was amplified with the following primers: BEko.α forward, 5′-GCTGGATCCAGCCTTCTCAAGGCTCAGTCATGCTCC-3′, and BEko.α reverse, 5′-ATGCGGCCGCAGTCTTCTCCAGGCTTTCATGCC-3′; BEko.β forward, 5′-GCGGCCGCATGTCTAACACTGCC-3′ and BEko.β reverse, 5′-ATGCGGCCGCGCATAAAAGTTTGTCTCAGG-3′. MSCV-IRES GFP(pMIG) vector was a gift from W. Sha (University of California, Berkeley). The BEko.α and BEko.β DNA fragments were cloned into the BamHI-NotI and NotI-NotI sites of the pMIG vector. Generation of retrovirus and transduction of suspension cells have been described (26).

Mice

The genomic DNA fragments encoding *TRBV5-TRBJ2-7* was amplified from BEko8Z with the following primers: 5′Primer: XholI-TRBV5-Fwd, 5′-TCTCTCGAGATGAGCTGCAGG-3′; 3′Primer: SacII-TRBJ2-7-Rev., 5′-CATGCCGCGGCACCACCCACC-3′. The DNA fragment was cloned into the cassette vector for TCR expression (27). The DNA construct was linearized and injected into fertilized (B6xSJL) F2 embryos. The transgenic founders were screened by amplification of the transgene with oligonucleotide primers described above. Transgene positive founders are backcrossed to C57BL/6 mice. ERAAP-KO, ERAAP-TAP-DKO mice have been described (21). Wild-type C57BL/6 were purchased from Jackson Laboratory. All experiments involving mice were done with the approval of Institutional Animal Care and Use Committee of the University of California, Berkeley.

Antibodies and cell lines

Antibodies for flow cytometry were from BD bioscience (anti-B220 (RA3-6B2), anti-CD3ε (145-2C11), anti-CD8α (53-6.7), anti-CD4 (RM4-5), anti-CD44 (IM7), anti-CD25 (PC61) anti-Vα3.2(RR3-16), anti-Vα8.3(B21.14), anti-Vα2 (B20.1), anti-Vβ5.1/5.2(MR9-4), anti-Vβ8.1/8.2(MR5-2), anti-Vβ3(KJ25), anti-Vβ2(B20.6), anti-Vβ8.3(1B3.3), anti-Vβ6(RR4-7), anti-Vβ7(TR310), anti-RORχT (Q31-378), anti-PLZF (R17-809)), eBiosciences (anti-TCRβ(H57-597), anti-T-bet (eBio4B10)) and BioLegend (anti-CD122 (TM-β1), anti-CD127 (A7R34)). The BEko.8Z hybridoma, C6VL.22α-, C6VL51.β- and 58α-β-mutant cell lines have been described earlier (21, 28).

Enrichment for tetramer-positive cells and flow cytometry

The Qa-1^{b}-FL9 monomers were obtained from the Tetramer Core Facility of the US National Institute of Health and tetramerized with phycoerythrin(PE)- or allophycocyanin(APC)-labeled streptavidin from Prozyme Advancing Glycosciences. Homogenized mice spleen cells were resuspended in 200ul of sorter's buffer (PBS with

2%FCS and 0.1% sodium azide) and stained with PE or APC labeled QFL tetramers at a final dilution of 1:200 and 1:100 at 23 °C for 50 min. QFL tetramer$^+$ T cells were enriched, gated and counted as described (21). The enriched fraction of cells was stained with anti-Vα3.2, anti-Vα8, anti-Vα2, anti-Vβ5.1/5.2, anti-Vβ8.1/8.2 and anti-Vβ2 for TCR analysis and anti-CD44, anti-CD122, anti-CD25 and anti-CD127 for surface marker characterization. For transcription factor staining, the enriched fraction of cells was first stained with anti-CD4, anti-B220, anti-CD8, anti-TCRβ and anti-CD44, fixed and permeabilized for 45 min and then stained with anti-T-bet, anti-RORχT and anti-PLZF for 45 min using BD transcription factor set. Cells were analyzed on Fortessa X20 and data was analyzed with FlowJo (TreeStar) software.

Single cell TCR analysis

The enriched QFL tetramer+ T cells from 3 mice were pooled and suspended in PBS PBS containing 2% BSA and 200 U RNAsin/ml (Promega) and sorted as single cells in to 96-well PCR plates using BD Influx Sorter. The multiplex nested RT-PCR protocol and the oligonucleotide primers used for CDR3 region amplification have been previously described (29). The sequence data has been deposited in GenBank (https://www.ncbi.nlm.nih.gov/genbank/) under accession numbers KY271957 and KY271958.

Results

TCR α- and β-chains expressed by T cell hybridoma specific for ERAAP-deficient cells

BEko8Z, a β-galactosidase(LacZ) inducible T cell hybridoma, was derived from C57BL/6 mice immunized with ERAAP-deficient cells (21). This hybridoma responds specifically to splenocytes from ERAAP-deficient mice but not to self-B6 splenocytes (Fig. 1a). Previous studies have also revealed that the ligand recognized by BEko8Z T cells is the FYAEATPML(FL9) peptide presented by Qa-1^b, the non-classical MHC Ib molecule and the Qa-1^b-FL9 complex is referred to as the QFL ligand (21). We first analyzed the TCR subunits used by the BEko8Z using a nested-PCR based strategy (29). The transcripts of the TCR α- and β-chain (BEko.α- and β-chain) were amplified simultaneously. We found that TRAV9d-3-TRAJ21 and TRBV5-TRBD1-TRBJ2-7 rearrangements were most likely used to encode the BEko.α and BEko.β chains. The full-length nucleotide sequence of BEko.α and BEko.β cDNA - determined using oligonucleotide primers specific for TRAV9d-3 and TRBV5 - revealed that the gene segments were productively rearranged (Fig. 1b). We concluded that TRAV9d-3-TRAJ21 (Vα3.2-Jα21) and TRBV5-TRBD1-TRBJ2-7 (Vβ1-Dβ1-Jβ2-7) were used to generate the full-length TCR α- and β-chains in BEko8Z T cells.

Structural features of the αβ TCR required for QFL ligand recognition

We next assessed whether the TCR α- and β-chains identified above recognized the Qa1-FL9 complex (QFL). The cDNAs were used to prepare constructs with the BEko.α and BEko.β cloned into a retroviral vector that also encoded the IRES-GFP cassette to allow identification of transfected cells. We transduced mutant T cell lines C6VL.22, C6VL.51 and 58α$^-$β$^-$ that lacked expression of endogenous TCR α- or TCR β-chain alone or both TCR α- and TCR β-chains. As a consequence none of these recipient cells expressed αβ TCR or the CD3 complex on the cell surface (28, 30). Among the GFP$^+$ transduced cells, the

TCR/CD3 expressing cells were obtained by sorting for the $CD3^+GFP^+$ population indicating that each TCR α- or β-chains successfully paired with its respective β or α counterpart as well as CD3 polypeptides (Fig. 2a). These $CD3^+$ cell lines were then stained with QFL-tetramer reagent prepared using the QFL-monomer obtained from the Tetramer Core Facility of the National Institutes of Health (21). The specificity of the QFL-tetramer was confirmed by staining BEko8Z T cells (Fig. 2b). However, despite high-levels of TCR/CD3 expression by all TCR transduced cells, only the $58\alpha^-\beta^-$ cells expressing both the BEko.α- and β-chains bound the QFL tetramer as compared to vector only control (Fig. 2b). The cells expressing either of the BEko.α- or β-chain paired with the endogenous β- or α-chain of the recipient cells did not stain with the fluorescent tetramer reagent. Thus, the QFL ligand recognition by the BEko.TCR required both the BEko.α- and BEko.β-chains.

The CDR3 regions, which comprise the junctions of the V(D)J on the TCR α- and β-chains are key elements that define the ligand specificity of the TCR (31, 32). To assess whether this canonical binding pattern applied to the BEko.TCR as well, we identified the CDR3 regions of BEko.α and BEko.β TCR chains by analyzing their DNA sequence using the IMGT database (http://www.imgt.org, (33)). The four and three amino acids respectively within the prospective CDR3 junctional region of BEko.α- and β-chain were replaced with alanine residues (Fig. 2c). The cell lines expressing BEko.α 4A or BEko.β 3A mutants paired with the wild-type BEko.β- or α-chain were generated by transducing the $58\alpha^-\beta^-$ cells described above. Again each α- and β-chain of TCRs paired with each other and the CD3 subunits (Fig. 2d). However, staining the GFP^+CD3^+ cells with the fluorescent QFL-tetramer showed that in contrast to cells expressing the wild-type BEko.TCR (α+β), tetramer binding was completely abolished in cells expressing either the 4A α-chain or the 3A β-chain mutants paired with their wild-type β or α counterpart (Fig. 2e). We conclude that the CDR3 regions on both the α- and β-chain of the BEko.TCR are essential for QFL ligand recognition.

QFL-specific T cells in BEko. β-chain transgenic mice

To assess the diversity of TCR α-chains that could be used to generate QFL-specific T cells *in vivo,* we generated transgenic mice expressing the BEko. β-chain (βTg). The rearranged genomic fragment encoding the *VDJ* segments of the BEko.β-chain was cloned into the TCRβ cassette vector and microinjected into fertilized eggs (Fig. 3a) (27). We identified four TCR transgenic mice by PCR amplification of the injected construct in tail DNA samples (Supplementary Fig S1a). The founder line #3 referred to as βTg was chosen for subsequent analysis because the transgene was well expressed and efficiently transmitted to the progeny. The fraction of $CD4^+$ and $CD8^+$ population as well as the total number of T cells were normal in βTg mice as compared with wild-type mice and the transgene negative littermates (Supplementary Fig. S1b). Analysis of $CD4^+$ and $CD8^+$ T cell subsets in thymocytes and splenocytes from the βTg mice with a set of TCR Vβ antibodies showed the expected staining in wild-type and transgene negative littermates (Supplementary Fig S1c). In contrast, these TCR $V\beta^+$ cells were not detected in βTg mice even though these mice contained cells expressing TCR β-chains detected by the antibody specific for the Cβ constant region. We conclude that transgene expression suppressed expression of diverse endogenous TCR β-chains leaving the T cells to pair the TCR β transgene with

endogenously rearranged TCR α-chains to allow development of normal number of $CD4^+$ and $CD8^+$ T cells.

We analyzed the QFL-specific T cells in βTg mice by staining splenocytes with QFL-tetramers labeled with two different fluorophores, followed by magnetic bead-based enrichment of the tetramer positive cells (34, 35). As observed earlier approximately 900 QFL-specific T cells were found per spleen in naïve wild-type mice (Fig. 3a) (21). In contrast, the number of QFL-specific T cells was enhanced about 7 fold to an average of 6,400 QFL-specific T cells in a naïve βTg spleen. As a negative control, QFL-specific T cells were undetectable in mice lacking the TAP transporter (Fig. 3b,c). We further analyzed QFL-specific T cells for CD44 expression, which was earlier shown to be expressed in a surprisingly high fraction of QFL-specific T cells in naive WT mice (21). We found ~86% of the QFL-specific T cells from naïve βTg mice were $CD44^{hi}$, which is substantially higher than the 48% frequency detected in naïve wild-type mice (Fig. 3d,e). In contrast, there was no significant difference between wild-type and the βTg mice in the frequency of $CD44^{hi}$ cells among all $CD8^+$ cells (Fig.3e). We infer that QFL-specific T cells developed robustly in βTg mice with a similar $CD44^{hi}$ antigen-experienced phenotype as in WT mice.

TCR α-chains of QFL-specific T cells in naïve βTg mice

To identify the corresponding TCR α-chains expressed by the QFL-specific T cells, we isolated single T cells by sorting the QFL-$tetramer^+$ T cells enriched from splenocytes of naïve βTg mice. The rearranged TCR α- and β-chain encoding mRNAs were then amplified from the sorted cells using the same multiplex nested-PCR protocol as above (29). Strikingly in ~98% (82/84) cells analyzed the TCR α-chain contained the TRAV9d-3 segment (Fig. 4a). Among these TRAV9d-3 Vα rearrangements, ~80% (66/82) were joined to the Jα segment TRAJ21. The remaining 16 TRAV9d-3 Vα as well as the two other Vα segments detected were rearranged to 9 distinct Jα segments (Fig. 4a). Strikingly, this dominant TCRα chain formed by the Vα-Jα rearrangement was virtually identical to the BEko.α-chain which was also formed by TRAV9d-3 rearranged with TRAJ21 and paired with the same BEko.β-chain encoded by the transgene (Fig. 4b and 1b). We further confirmed the high frequency of cells expressing TRAV9 by staining the QFL-specific T cells with antibodies specific for different TRAV regions (36, 37). Consistent with the result from the single cell TCR analysis, about 98% of the QFL-specific T cells were stained with anti-TRAV9 antibody compared to <2% of $TRAV9^+$ cells among all $CD8^+$ T cells (Fig. 4 c,d). By contrast, TRAV12 or TRAV14 expressing cells were barely detectable among the QFL-tetramer positive cells. We conclude that the QFL-specific T cells in βTg mice expressing a single TCRβ chain developed using a predominant and unique Vα-Jα rearrangement of TCR α-chains.

Interestingly, among the 66 cells that had the TRAV9d-3-TRAJ21 rearrangement, 12 cells were identified with variations within the CDR3 region while the remaining 54 cells expressed the TCR α-chain identical to BEko.α. We noted that the first valine (V) in the CDR3 region was occasionally substituted with alanine (A, 7/66), threonine (T, 2/66) or serine (S, 1/66). Likewise, the second serine (S) residue was substituted by asparagine (N) residue in 2/66 sequences (Fig. 4e). To test the functional significance of these substitutions,

we generated GFP fusion constructs encoding TCRα with these two amino acid substitutions as well as alanine substitutions for each of the other three amino acids within the junctional CDR3 region (Fig. 4f). The TCRα mutants together with the wild-type BEko.β-chain were introduced into 58α $^{-}$β $^{-}$ cells that lacked endogenous TCRα- and TCR β-chains as above. The TCR^{+} cells were sorted by flow cytometry as CD3^{+}GFP^{+} population and tested for their ability to bind the QFL-tetramer (Fig. 4g). The cells that expressed the two natural variants (V>A or V>T) of BEko.α-chain bound the QFL-tetramer as well as the ones that expressed the BEko.α-chain. In contrast, substitution of the other amino acids within the junctional region either partially or completely disrupted ligand recognition (Fig. 4h). We conclude that in βTg mice, the QFL-specific T cells not only express predominantly invariant Vα and Jα segments, but also a near invariant junctional CDR3 region for recognizing the QFL ligand.

TCR analysis of QFL-specific T cells in naïve wild-type mice

To determine the natural diversity among the TCR α- and β-chains of QFL-specific T cells, we analyzed splenocytes of naïve wild-type mice. The single cells were obtained and analyzed using methods similar to those used for the βTg mice described above. We found that the TRAV9d-3 and TRAJ21 used by the BEko.α-chain were again the most frequent Vα-Jα rearrangement. About 84% (42/50) of the cells analyzed used the TRAV9d-3 Vα segment and 36% (18/50) of these used the TRAJ21 Jα segment (Fig. 5a). Virtually all the Vα-Jα rearrangements had the same CDR3 junction identical to that of BEko.α chain with the exception of a single CDR3 that contained a valine to alanine substitution (Fig 5b). The remaining TRAV9d-3 Vα as well as the six other Vα segments detected were joined to 22 different Jα segments (Fig. 5a). Thus the TCR repertoire of QFL-specific T cells is somewhat more diverse in wild-type relative to βTg mice. Staining of the enriched QFL-specific T cells with antibodies specific for different Vα regions showed that about 80% of the QFL-specific T cells expressed TRAV9, relative to a few (~3%) of TRAV12^{+} cells that were also detected. However, as a negative control TRAV14^{+} cells remained undetectable (Fig. 5c). In contrast the frequency of cells that used each of the three TRAVs in total CD8^{+} T cell population was about 4% (Fig. 5d). We conclude that similar to the BEko8Z hybridoma and T cells in βTg mice, the QFL-specific T cells in wild-type mice also used the TRAV9d-3 Vα segment that was most frequently rearranged to the TRAJ21 Jα segment.

The β-chains pairing with these α-chains were then similarly assessed for the Vβ and Jβ usage in the same cells. We found TRBV5 - the Vβ segment used by BEko.β - was used by 40% (20/50) of the QFL-specific cells analyzed (Fig. 6a and Fig. 1b). Likewise, the TRBJ2-7 - also the Jβ used by BEko.β - was used by 50% (25/50) of wild-type cells. Thus, in about 40% (20/50) of TCR β-chains, TRBV5 was joined to the TRBJ2-7 segment as the predominant rearrangement similar to the BEko.β TCR chain. All the TCR β-chains that were identical to BEko.β-chains were paired exclusively to the TCR α-chain identical to BEko.α (Fig. 6b). Two variations of amino acid sequence within CDR3 were detected in 3 of the cells that used the TRBV5-TRBJ2-7 rearrangement. Unlike the single amino acid substitution found in the α-chains, the junctional region of CDR3 were substantially altered among TCR β-chain variants. But none of the 3 variants were paired with the BEko.α-chain (Fig. 6c). A relatively high frequency of TCR β-chains also used TRBV12-1/12-2

rearranged to a diversity of TRBJs. About 32% (16/50) of the QFL-specific T cells expressed TRBV12-2/12-1 and 4% (2/50) used TRBV26 (Fig. 6a). This was directly confirmed by staining the QFL-specific T cells with antibodies specific for different TRBVs. The QFL-specific T cell population contained ~30% cells that stained with the anti-TRBV12-2/12-1 antibody, 1.8% that stained with the anti-TRBV26 antibody, but TRBV13-3/13-2^{+} cells were undetectable (Fig. 6d and e). Although antibody specific for TRBV5 is not available, we deduced that the ~70% TRBV12^{-} cells include the TRBV5^{+} cells. We conclude that in wild-type mice, the QFL-specific T cells comprise a major subset bearing the invariant TCR α- and β-chains and a minor subset bearing the same TRAV9 Vα segment but rearranged to a variety of other TRAJ segments. These TCR α chains are paired with a limited number of TCR β-chains such as TRBV5 and TRBV12-2/12-1 joined with several distinct TRBJs.

Characterization of QFL-specific T cells in naïve mice

The predominant use of a particular TCR α-chain and limited TCR β-chains by QFL-specific T cells suggested a striking similarity of QFL-TCRs with TCRs used by the iNKT and MAIT cell subsets. Notably, the iNKT and MAIT cells also predominantly use highly invariant TCR α-chains and a limited number of TCR β-chains (39). The iNKT cells are also characterized by their memory-like and 'poised effector' phenotype (40, 41). We therefore further investigated the expression of iNKT surface markers and transcription factors by the QFL-specific T cells. The enriched QFL-specific T cell population was assessed for CD44, CD122, CD25 and CD127 expression by flow cytometry. We found that the CD44^{hi}CD122^{hi} antigen experienced T cells were present at a ~15% higher frequency in the CD8^{+}QFL^{+} population as compared to the CD8^{+}QFL^{-} population (Fig. 7a and b). This observation was further supported by the somewhat higher level of CD25 and CD127 expressed on the CD8^{+}QFL^{+} T cells compared to the CD8^{+}QFL^{-} T cells, suggesting that this population of T cells had the phenotype of readily activated, long-living memory T cells (42) (Fig. 7c and d). It has been proposed that the iNKT cell population can be subdivided into Th1-like, Th2-like and Th17-like cells based on the expression of the 'master' regulators, T-bet, PLZF and RORχT (40). We thus assessed expression of these transcriptional factors in QFL-specific T cells. Remarkably, we found that the CD44^{hi}QFL^{+} T cells were distinguished by the T-bet^{+} but PLZF^{-}RORχT^{-} expression pattern, as compared to the CD44^{hi}NK1.1^{+} cell subset that contained cells expressing each of the three transcription factors (Fig. 7e and f). This observation agrees with the CD122^{hi} phenotype of the QFL-specific T cells and our previously reported observation of a substantial fraction of the QFL^{+} T cells producing IFNχ in response to the ERAAP-ko APCs (21). We conclude that the majority of QFL-specific T cells share some characteristics with antigen-experienced and effector memory-like T cells.

Discussion

Conventional CD8^{+} T cell responses are initiated by specific recognition of the pMHC Ia complex on the surface of antigen presenting cells. The diversity of αβ TCRs that recognize a particular pMHC Ia complex is the defining property of most conventional CD8^{+} T cell responses. Here we described a unique population of CD8^{+} T cells that express semi-

invariant TCRs to monitor ERAAP-deficiency by recognizing a conserved peptide presented by Qa-1^b, a non-classical MHC Ib molecule. These TCR and ligand characteristics together with their high frequency and antigen-experienced phenotype in naive mice makes the QFL-specific $CD8^+$ T cells uniquely different from conventional pMHC Ia restricted $CD8^+$ T cells but akin to innate-like T cells.

We analyzed the αβ TCRs expressed by the BEko8Z hybridoma that was originally generated by fusing anti-ERAAP specific $CD8^+$ T cells with a fusion partner lacking endogenous αβ TCR (21, 43). This lacZ inducible hybridoma was used earlier to identify the QFL ligand that was induced by ERAAP-deficiency. The QFL was the immunodominant ligand that elicited $CD8^+$ T cells in wild-type mice by ERAAP-deficient cells. Remarkably, the TCR α- and β-chains from this hybridoma were also commonly expressed by other QFL-specific $CD8^+$ T cells in naive wild-type mice and by virtually all QFL-specific $CD8^+$ T cells in TCR β-chain transgenic mice. The Vα segment TRAV9d-3 rearranged to the TRAJ21 Jα segment was therefore the most prevalent among all TCR α-chains expressed by QFL-specific T cells. Likewise, the TRBV5 encoded Vβ segment dominated the TCR β chains, but other TRBV12-1/12-2 rearrangements were also used by a substantial fraction of T cells. Altogether, the results show that the QFL-specific T cells express a nearly invariant TCR α-chain and a dominant but not exclusive TCR β-chain. Thus, the QFL-specific T cells contain a major subset of invariant αβ TCR as well as a minor more diverse set of αβ TCRs. Both TCRs recognize the same QFL ligand, but whether the receptor contacts with the ligand similarly is not yet known.

Interesting parallels emerge when the QFL-specific αβ TCRs are compared with other TCRs that are also restricted by different non-classical MHC Ib molecules. The iNKT and MAIT cells also bear semi-invariant receptors with invariant TCR α-chains and a limited set of TCR β-chains (39, 44). These TCRs recognize MHC Ib molecules CD1d or MR1 presenting glycolipids or vitamin B metabolites respectively (23, 45, 46). Structural analysis has revealed that the orientation of type I iNKT TCRs positioned on CD1d-antigen surface is distinct from the conventional diagonal TCR-binding mode for classical pMHC I-TCR recognition (47). Because of the positioning of iNKT TCR, the invariant TCR α-chain predominantly contacts the CD1d ligand and determines ligand recognition with variable TCR β-chains. The interaction between the invariant TCR α-chain and the ligand is mainly mediated by the CDR3 region with emphasis on the Jα segment (48–50). On the other hand, the MAIT TCRs, although positioned in the classical diagonal TCR-binding mode, contact the MR1 ligands mainly through the invariant TCR α-chain (51, 52). The structure of the αβ TCR complexed with its QFL ligand is not yet known. Nevertheless, we found that the CDR3 regions of both the TCR α and β chains were essential for QFL binding. Furthermore, the Jα segment was important for ligand specificity because amino acid substitutions in this segment resulted in complete loss of ligand recognition. Thus, the QFL-specific TCRs appear structurally related to the iNKT TCRs.

The rearrangement of particular TCR α segments has revealed an unusual developmental pathway for iNKT and MAIT cells (39, 53). In both lineages the canonical TCR α-chain uses a distal Vα (TRAV11 or TRAV1) and a proximal Jα (TRAJ18 or TRAJ33) segment relative to the constant α gene segment. This configuration of Vα-Jα gene segments

suggested that the invariant TCR α-chains could arise by secondary TCR α rearrangements in immature T cells (54). Indeed development of the iNKT and MAIT cell lineages depends upon the master transcriptional regulators (HEB and RORχt) that prolong the time window available for continuing TCR α rearrangements by inducing expression of the anti-apoptotic factors such as Bcl-xL (55–57). Remarkably, the invariant TCR α-chain in QFL-specific T cells is also generated by rearrangement of another distal TRAV9d-3 Vα segment to the proximal TRAJ21 Jα segment. Thus it is likely that the TCR α chains in QFL-specific T cells would also occur late in development. Furthermore, it is well established that iNKT, MAIT as well as $CD8^+$ T cells restricted by H2-M3 MHC Ib molecules are positively selected by recognizing CD1d, MR-1 or H2-M3 expressed by double positive cells in the thymus and mature into cells that can rapidly secrete cytokines when stimulated in the periphery (55, 56, 58). Whether the QFL-specific T cells develop in a similar manner or function as cytokine producers in discrete anatomical locations is unknown.

In addition to the semi-invariant TCRs, the QFL-specific T cells are similar in some but not all characteristics of the iNKT and MAIT cells. We found that a large fraction of the QFL-specific T cells was $CD44^{hi}CD122^{hi}$ and expressed higher levels of CD25 and CD127 markers, which indicates these cells are readily activated and antigen experienced. Interestingly, unlike the innate-like NKT cell subset that is comprised of cell populations that express each of the three master regulators T-bet, PLZF or RORχT, the $CD44^{hi}$ QFL-specific T cells expressed $T\text{-}bet^+$ but essentially lacked expression of PLZF or RORχT. Together with our previously reported observation that these cells produce IFNχ and are cytotoxic towards ERAAP-deficient target cells, we speculate that the QFL-specific T cells are likely innate-like cytotoxic $CD8^+$ T cells. Despite the clear functional differences in cytokine secretion profiles versus cytotoxicity, the iNKT, MAIT and QFL-specific T cells may nevertheless share similarities in their developmental pathways.

In conclusion, we have identified a novel $CD8^+$ T cell population whose specificity is restricted by the non-classical Qa-1 MHC Ib molecule. These cells express a semi-invariant αβ TCRs similar to those expressed by the iNKT and MAIT cells restricted by other non-classical CD1d and MR1 MHC Ib molecules. Note the non-polymorphic MHC Ib molecules pre-date the classical, highly polymorphic MHC Ia molecules in evolution and bridge the innate and adaptive immune systems (38). Thus, unraveling the developmental pathway and functional properties of QFL-specific T cells in immune surveillance of ERAAP-deficiency should be interesting.

Supplementary Material

Refer to Web version on PubMed Central for supplementary material.

Acknowledgments

We thank the late Chulho Kang, Hector Nolla and Alma Valeros from the Cancer Research Laboratory for help in generating the transgenic mice and flow cytometry. This research was supported by grants from the NIAID and the NIH. JG was supported by grant from Chinese Scholarship Council.

References

1. Shastri N, Schwab S, Serwold T. Producing nature's gene-chips. The generation of peptides for display by MHC class I molecules. Annu Rev Immunol. 2002; 20:463–493. [PubMed: 11861610]
2. Blum JS, Wearsch PA, Cresswell P. Pathways of antigen processing. Annu Rev Immunol. 2013; 31:443–473. [PubMed: 23298205]
3. Neefjes J, Jongsma ML, Paul P, Bakke O. Towards a systems understanding of MHC class I and MHC class II antigen presentation. Nat Rev Immunol. 2011; 11:823–836. [PubMed: 22076556]
4. Shastri N, Cardinaud S, Schwab SR, Serwold T, Kunisawa J. All the peptides that fit: the beginning, the middle, and the end of the MHC class I antigen-processing pathway. Immunol Rev. 2005; 207:31–41. [PubMed: 16181325]
5. Rock KL, Farfan-Arribas DJ, Colbert JD, Goldberg AL. Re-examining class-I presentation and the DRiP hypothesis. Trends Immunol. 2014; 35:144–152. [PubMed: 24566257]
6. Van Kaer L, Ashton-Rickardt PG, Ploegh HL, Tonegawa S. TAP1 mutant mice are deficient in antigen presentation, surface class I molecules, and CD4-8+ T cells. Cell. 1992; 71:1205–1214. [PubMed: 1473153]
7. Serwold T, Gonzalez F, Kim J, Jacob R, Shastri N. ERAAP customizes peptides for MHC class I molecules in the endoplasmic reticulum. Nature. 2002; 419:480–483. [PubMed: 12368856]
8. Saric T, Chang SC, Hattori A, York IA, Markant S, Rock KL, Tsujimoto M, Goldberg AL. An IFN-g-induced aminopeptidase in the ER, ERAP1, trims precursors to MHC class I-presented peptides. Nature Immunology. 2002; 3:1169–1176. [PubMed: 12436109]
9. Van Kaer L, Ashton-Rickardt PG, Eichelberger M, Gaczynska M, Nagashima K, Rock KL, Goldberg AL, Doherty P, Tonegawa S. Altered peptidase and viral specific T cell response in LMP2 mutant mice. Immunity. 1994; 1:533–541. [PubMed: 7600282]
10. Grandea AG, Golovina TN, Hamilton SE, Sriram V, Spies T, Brutkiewicz RR, Harty JT, Eisenlohr LC, Van Kaer L. Impaired assembly yet normal trafficking of MHC class I molecules in tapasin mutant mice. Immunity. 2000; 13:213–222. [PubMed: 10981964]
11. Hammer GE, Gonzalez F, James E, Nolla H, Shastri N. In the absence of aminopeptidase ERAAP, MHC class I molecules present many unstable and highly immunogenic peptides. Nat Immunol. 2007; 8:101–108. [PubMed: 17128277]
12. Blanchard N, Shastri N. Coping with loss of perfection in the MHC class I peptide repertoire. Curr Opin Immunol. 2008; 20:82–88. [PubMed: 18243675]
13. Kincaid EZ, Che JW, York I, Escobar H, Reyes-Vargas E, Delgado JC, Welsh RM, Karow ML, Murphy AJ, Valenzuela DM, Yancopoulos GD, Rock KL. Mice completely lacking immunoproteasomes show major changes in antigen presentation. Nature Immunology. 2012; 13:129–135.
14. York IA, Chang SC, Saric T, Keys JA, Favreau JM, Goldberg AL, Rock KL. The ER aminopeptidase ERAP1 enhances or limits antigen presentation by trimming epitopes to 8–9 residues. Nat Immunol. 2002; 3:1177–1184. [PubMed: 12436110]
15. Yan J V, Parekh V, Mendez-Fernandez Y, Olivares-Villagomez D, Dragovic S, Hill T, Roopenian DC, Joyce S, Van Kaer L. In vivo role of ER-associated peptidase activity in tailoring peptides for presentation by MHC class Ia and class Ib molecules. J Exp Med. 2006; 203:647–659. [PubMed: 16505142]
16. York IA, Brehm MA, Zendzian S, Towne CF, Rock KL. Endoplasmic reticulum aminopeptidase 1 (ERAP1) trims MHC class I-presented peptides in vivo and plays an important role in immunodominance. Proc Natl Acad Sci USA. 2006; 103:9202–9207. [PubMed: 16754858]
17. Firat E, Saveanu L, Aichele P, Staeheli P, Huai J, Gaedicke S, Nil A, Besin G, Kanzler B, van Endert P, Niedermann G. The role of endoplasmic reticulum-associated aminopeptidase 1 in immunity to infection and in cross-presentation. J Immunol. 2007; 178:2241–2248. [PubMed: 17277129]
18. Fruci D, Giacomini P, Nicotra MR, Forloni M, Fraioli R, Saveanu L, van Endert P, Natali PG. Altered expression of endoplasmic reticulum aminopeptidases ERAP1 and ERAP2 in transformed non-lymphoid human tissues. J Cell Physiol. 2008; 216:742–749. [PubMed: 18393273]

19. Strange A, Capon F, Spencer CC, Knight J, Weale ME, Allen MH, Barton A, Band G, Bellenguez C, Bergboer JG, Blackwell JM, Bramon E, Bumpstead SJ, Casas JP, Cork MJ, Corvin A, Deloukas P, Dilthey A, Duncanson A, Edkins S, Estivill X, Fitzgerald O, Freeman C, Giardina E, Gray E, Hofer A, Huffmeier U, Hunt SE, Irvine AD, Jankowski J, Kirby B, Langford C, Lascorz J, Leman J, Leslie S, Mallbris L, Markus HS, Mathew CG, McLean WH, McManus R, Mossner R, Moutsianas L, Naluai AT, Nestle FO, Novelli G, Onoufriadis A, Palmer CN, Perricone C, Pirinen M, Plomin R, Potter SC, Pujol RM, Rautanen A, Riveira-Munoz E, Ryan AW, Salmhofer W, Samuelsson L, Sawcer SJ, Schalkwijk J, Smith CH, Stahle M, Su Z, Tazi-Ahnini R, Traupe H, Viswanathan AC, Warren RB, Weger W, Wolk K, Wood N, Worthington J, Young HS, Zeeuwen PL, Hayday A, Burden AD, Griffiths CE, Kere J, Reis A, McVean G, Evans DM, Brown MA, Barker JN, Peltonen L, Donnelly P, Trembath RC. A genome-wide association study identifies new psoriasis susceptibility loci and an interaction between HLA-C and ERAP1. Nature Genetics. 2010; 42:985–990. [PubMed: 20953190]

20. Evans DM, Spencer CC, Pointon JJ, Su Z, Harvey D, Kochan G, Oppermann U, Dilthey A, Pirinen M, Stone MA, Appleton L, Moutsianas L, Leslie S, Wordsworth T, Kenna TJ, Karaderi T, Thomas GP, Ward MM, Weisman MH, Farrar C, Bradbury LA, Danoy P, Inman RD, Maksymowych W, Gladman D, Rahman P, Morgan A, Marzo-Ortega H, Bowness P, Gaffney K, Gaston JS, Smith M, Bruges-Armas J, Couto AR, Sorrentino R, Paladini F, Ferreira MA, Xu H, Liu Y, Jiang L, Lopez-Larrea C, Diaz-Pena R, Lopez-Vazquez A, Zayats T, Band G, Bellenguez C, Blackburn H, Blackwell JM, Bramon E, Bumpstead SJ, Casas JP, Corvin A, Craddock N, Deloukas P, Dronov S, Duncanson A, Edkins S, Freeman C, Gillman M, Gray E, Gwilliam R, Hammond N, Hunt SE, Jankowski J, Jayakumar A, Langford C, Liddle J, Markus HS, Mathew CG, McCann OT, McCarthy MI, Palmer CN, Peltonen L, Plomin R, Potter SC, Rautanen A, Ravindrarajah R, Ricketts M, Samani N, Sawcer SJ, Strange A, Trembath RC, Viswanathan AC, Waller M, Weston P, Whittaker P, Widaa S, Wood NW, McVean G, Reveille JD, Wordsworth BP, Brown MA, Donnelly P. Interaction between ERAP1 and HLA-B27 in ankylosing spondylitis implicates peptide handling in the mechanism for HLA-B27 in disease susceptibility. Nat Genet. 2011; 43:761–767. [PubMed: 21743469]

21. Nagarajan NA, Gonzalez F, Shastri N. Nonclassical MHC class Ib-restricted cytotoxic T cells monitor antigen processing in the endoplasmic reticulum. Nat Immunol. 2012; 13:579–586. [PubMed: 22522492]

22. Turner SJ, Doherty PC, McCluskey J, Rossjohn J. Structural determinants of T-cell receptor bias in immunity. Nature reviews Immunology. 2006; 6:883–894.

23. Lantz O, Bendelac A. An invariant T cell receptor alpha chain is used by a unique subset of major histocompatibility complex class I-specific CD4+ and CD4-8- T cells in mice and humans. The Journal of experimental medicine. 1994; 180:1097–1106. [PubMed: 7520467]

24. Tilloy F, Treiner E, Park SH, Garcia C, Lemonnier F, de la Salle H, Bendelac A, Bonneville M, Lantz O. An invariant T cell receptor alpha chain defines a novel TAP-independent major histocompatibility complex class Ib-restricted alpha/beta T cell subpopulation in mammals. J Exp Med. 1999; 189:1907–1921. [PubMed: 10377186]

25. Reantragoon R, Kjer-Nielsen L, Patel O, Chen Z, Illing PT, Bhati M, Kostenko L, Bharadwaj M, Meehan B, Hansen TH, Godfrey DI, Rossjohn J, McCluskey J. Structural insight into MR1-mediated recognition of the mucosal associated invariant T cell receptor. J Exp Med. 2012; 209:761–774. [PubMed: 22412157]

26. Swift S, Lorens J, Achacoso P, Nolan GP. Rapid production of retroviruses for efficient gene delivery to mammalian cells using 293T cell-based systems. Curr Protoc Immunol Chapter. 2001; 10(Unit 10.17C)

27. Kouskoff V, Signorelli K, Benoist C, Mathis D. Cassette vectors directing expression of T cell receptor genes in transgenic mice. J Immunol Methods. 1995; 180:273–280. [PubMed: 7714342]

28. Glaichenhaus N, Davis C, Bornschlegel K, Allison JP, Shastri N. A novel strategy for the generation of T cell lines lacking expression of endogenous alpha- and/or beta-chain T cell receptor genes. J Immunol. 1991; 146:2095–2101. [PubMed: 1826016]

29. Dash P, McClaren JL, Oguin TH 3rd, Rothwell W, Todd B, Morris MY, Becksfort J, Reynolds C, Brown SA, Doherty PC, Thomas PG. Paired analysis of TCRalpha and TCRbeta chains at the single-cell level in mice. J Clin Invest. 2011; 121:288–295. [PubMed: 21135507]

30. Letourneur F, Malissen B. Derivation of a T cell hybridoma variant deprived of functional T cell receptor alpha and beta chain transcripts reveals a nonfunctional alpha-mRNA of BW5147 origin. European Journal of Immunology. 1989; 19:2269–2274. [PubMed: 2558022]
31. Davis MM, Bjorkman PJ. T-cell antigen receptor genes and T-cell recognition. Nature. 1988; 334:395–402. [PubMed: 3043226]
32. Rossjohn J, Gras S, Miles JJ, Turner SJ, Godfrey DI, McCluskey J. T cell antigen receptor recognition of antigen-presenting molecules. Annu Rev Immunol. 2015; 33:169–200. [PubMed: 25493333]
33. Lefranc MP, Giudicelli V, Ginestoux C, Jabado-Michaloud J, Folch G, Bellahcene F, Wu Y, Gemrot E, Brochet X, Lane J, Regnier L, Ehrenmann F, Lefranc G, Duroux P. IMGT, the international ImMunoGeneTics information system. Nucleic Acids Res. 2009; 37:D1006–1012. [PubMed: 18978023]
34. Moon JJ, Chu HH, Pepper M, McSorley SJ, Jameson SC, Kedl RM, Jenkins MK. Naive CD4(+) T cell frequency varies for different epitopes and predicts repertoire diversity and response magnitude. Immunity. 2007; 27:203–213. [PubMed: 17707129]
35. Moon JJ, Chu HH, Hataye J, Pagan AJ, Pepper M, McLachlan JB, Zell T, Jenkins MK. Tracking epitope-specific T cells. Nat Protoc. 2009; 4:565–581. [PubMed: 19373228]
36. Utsunomiya Y, Bill J, Palmer E, Gollob K, Takagaki Y, Kanagawa O. Analysis of a monoclonal rat antibody directed to the alpha-chain variable region (V alpha 3) of the mouse T cell antigen receptor. J Immunol. 1989; 143:2602–2608. [PubMed: 2477449]
37. Pircher H, Rebai N, Groettrup M, Gregoire C, Speiser DE, Happ MP, Palmer E, Zinkernagel RM, Hengartner H, Malissen B. Preferential positive selection of V alpha 2+ CD8+ T cells in mouse strains expressing both H-2k and T cell receptor V alpha a haplotypes: determination with a V alpha 2-specific monoclonal antibody. Eur J Immunol. 1992; 22:399–404. [PubMed: 1311260]
38. Rodgers JR, Cook RG. MHC class Ib molecules bridge innate and acquired immunity. Nat Rev Immunol. 2005; 5:459–471. [PubMed: 15928678]
39. Salio M, Silk JD, Jones EY, Cerundolo V. Biology of CD1- and MR1-restricted T cells. Annu Rev Immunol. 2014; 32:323–366. [PubMed: 24499274]
40. Brennan PJ, Brigl M, Brenner MB. Invariant natural killer T cells: an innate activation scheme linked to diverse effector functions. Nat Rev Immunol. 2013; 13:101–117. [PubMed: 23334244]
41. Godfrey DI, Stankovic S, Baxter AG. Raising the NKT cell family. Nat Immunol. 2010; 11:197–206. [PubMed: 20139988]
42. Huster KM, Busch V, Schiemann M, Linkemann K, Kerksiek KM, Wagner H, Busch DH. Selective expression of IL-7 receptor on memory T cells identifies early CD40L-dependent generation of distinct CD8+ memory T cell subsets. Proc Natl Acad Sci U S A. 2004; 101:5610–5615. [PubMed: 15044705]
43. Sanderson S, Shastri N. LacZ inducible, antigen/MHC-specific T cell hybrids. Int Immunol. 1994; 6:369–376. [PubMed: 8186188]
44. Bendelac A, Savage PB, Teyton L. The biology of NKT cells. Annual review of immunology. 2007; 25:297–336.
45. Rossjohn J, Pellicci DG, Patel O, Gapin L, Godfrey DI. Recognition of CD1d-restricted antigens by natural killer T cells. Nat Rev Immunol. 2012; 12:845–857. [PubMed: 23154222]
46. Godfrey DI, Uldrich AP, McCluskey J, Rossjohn J, Moody DB. The burgeoning family of unconventional T cells. Nat Immunol. 2015; 16:1114–1123. [PubMed: 26482978]
47. Borg NA, Wun KS, Kjer-Nielsen L, Wilce MC, Pellicci DG, Koh R, Besra GS, Bharadwaj M, Godfrey DI, McCluskey J, Rossjohn J. CD1d-lipid-antigen recognition by the semi-invariant NKT T-cell receptor. Nature. 2007; 448:44–49. [PubMed: 17581592]
48. Mallevaey T, Scott-Browne JP, Matsuda JL, Young MH, Pellicci DG, Patel O, Thakur M, Kjer-Nielsen L, Richardson SK, Cerundolo V, Howell AR, McCluskey J, Godfrey DI, Rossjohn J, Marrack P, Gapin L. T cell receptor CDR2 beta and CDR3 beta loops collaborate functionally to shape the iNKT cell repertoire. Immunity. 2009; 31:60–71. [PubMed: 19592274]
49. Pellicci DG, Patel O, Kjer-Nielsen L, Pang SS, Sullivan LC, Kyparissoudis K, Brooks AG, Reid HH, Gras S, Lucet IS, Koh R, Smyth MJ, Mallevaey T, Matsuda JL, Gapin L, McCluskey J, Godfrey DI, Rossjohn J. Differential recognition of CD1d-alpha-galactosyl ceramide by the V beta

8.2 and V beta 7 semi-invariant NKT T cell receptors. Immunity. 2009; 31:47–59. [PubMed: 19592275]

50. Patel O, Pellicci DG, Uldrich AP, Sullivan LC, Bhati M, McKnight M, Richardson SK, Howell AR, Mallevaey T, Zhang J, Bedel R, Besra GS, Brooks AG, Kjer-Nielsen L, McCluskey J, Porcelli SA, Gapin L, Rossjohn J, Godfrey DI. Vbeta2 natural killer T cell antigen receptor-mediated recognition of CD1d-glycolipid antigen. Proc Natl Acad Sci U S A. 2011; 108:19007–19012. [PubMed: 22065767]
51. Patel O, Kjer-Nielsen L, Le Nours J, Eckle SB, Birkinshaw R, Beddoe T, Corbett AJ, Liu L, Miles JJ, Meehan B, Reantragoon R, Sandoval-Romero ML, Sullivan LC, Brooks AG, Chen Z, Fairlie DP, McCluskey J, Rossjohn J. Recognition of vitamin B metabolites by mucosal-associated invariant T cells. Nat Commun. 2013; 4:2142. [PubMed: 23846752]
52. Lopez-Sagaseta J, Dulberger CL, Crooks JE, Parks CD, Luoma AM, McFedries A, Van Rhijn I, Saghatelian A, Adams EJ. The molecular basis for Mucosal-Associated Invariant T cell recognition of MR1 proteins. Proc Natl Acad Sci U S A. 2013; 110:E1771–1778. [PubMed: 23613577]
53. Engel I, Kronenberg M. Transcriptional control of the development and function of Valpha14i NKT cells. Curr Top Microbiol Immunol. 2014; 381:51–81. [PubMed: 24839184]
54. Engel I, Kronenberg M. Making memory at birth: understanding the differentiation of natural killer T cells. Curr Opin Immunol. 2012; 24:184–190. [PubMed: 22305304]
55. Bezbradica JS, Hill T, Stanic AK, Van Kaer L, Joyce S. Commitment toward the natural T (iNKT) cell lineage occurs at the CD4+8+ stage of thymic ontogeny. Proc Natl Acad Sci U S A. 2005; 102:5114–5119. [PubMed: 15792999]
56. Egawa T, Eberl G, Taniuchi I, Benlagha K, Geissmann F, Hennighausen L, Bendelac A, Littman DR. Genetic evidence supporting selection of the Valpha14i NKT cell lineage from double-positive thymocyte precursors. Immunity. 2005; 22:705–716. [PubMed: 15963785]
57. D'Cruz LM, Knell J, Fujimoto JK, Goldrath AW. An essential role for the transcription factor HEB in thymocyte survival, Tcra rearrangement and the development of natural killer T cells. Nat Immunol. 2010; 11:240–249. [PubMed: 20154672]
58. Urdahl KB, Sun JC, Bevan MJ. Positive selection of MHC class Ib-restricted CD8(+) T cells on hematopoietic cells. Nat Immunol. 2002; 3:772–779. [PubMed: 12089507]

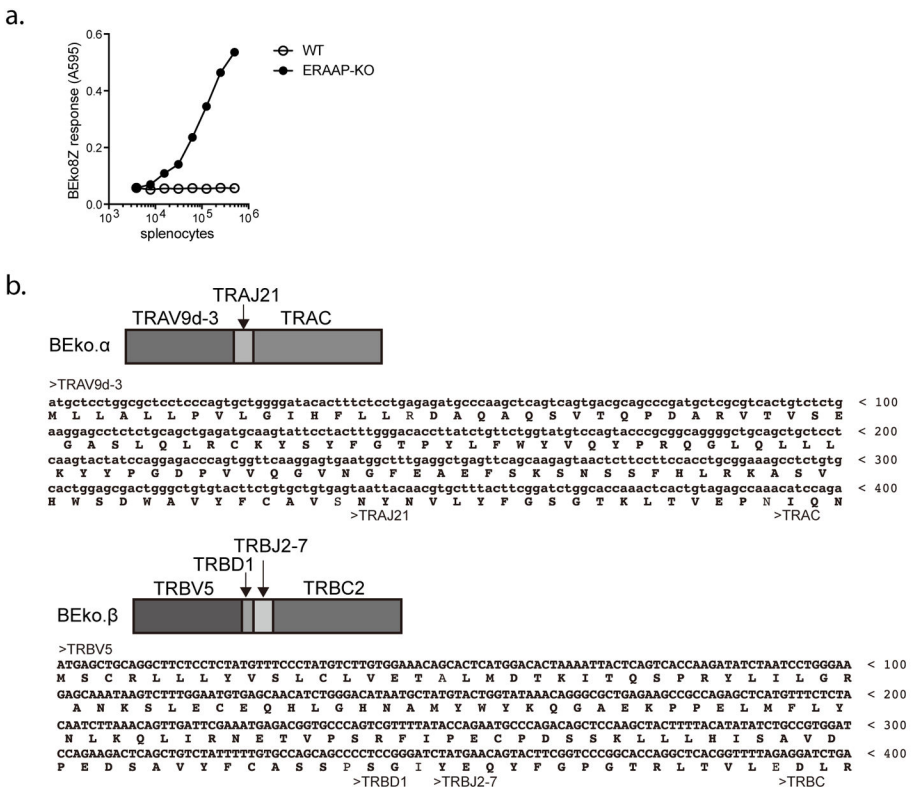

Figure 1.

The sequence of αβ TCR expressed by BEko8Z hybridoma. (a) Specificity of BEko8Z hybridoma. The LacZ response of BEko8Z hybridoma cells to varying number of WT or ERAAP-KO spleen cells was measured by absorbance (A595) of the cleaved lacZ substrate chlorophenol red β-D-galactopyrandoside. Data is representative of three independent experiments. (b) Schematic structure, the nucleotide and the translated amino acid sequences of the TCR α (BEko.α) and β (BEko.β) chains. Annotations above and below the sequence show the various rearranged V, D and J segments for the alpha and beta chains.

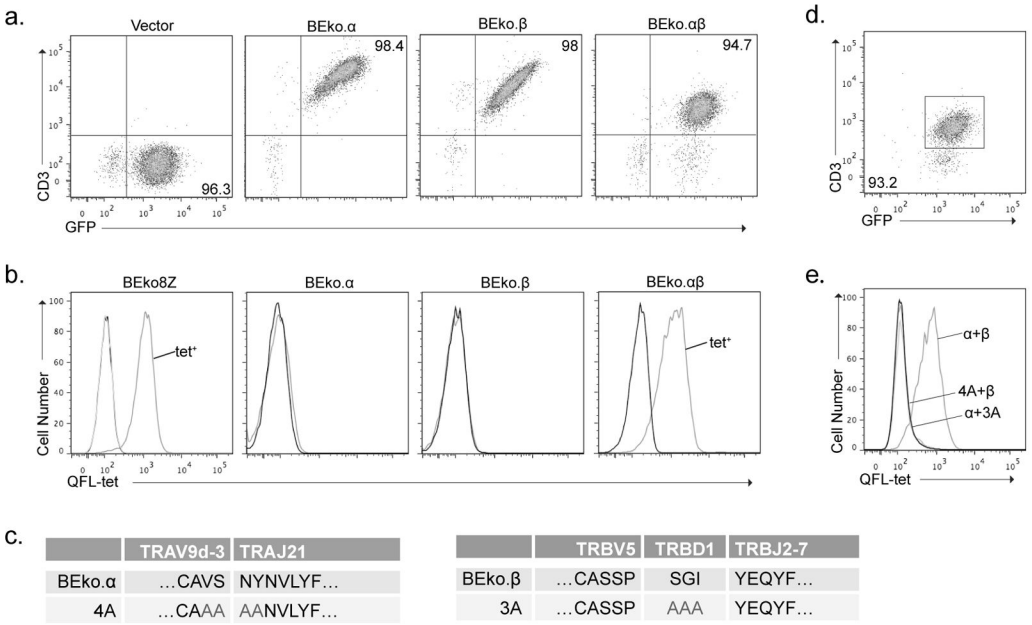

c.

	TRAV9d-3	TRAJ21
BEko.α	…CAVS	NYNVLYF…
4A	…CAAA	AANVLYF…

	TRBV5	TRBD1	TRBJ2-7
BEko.β	…CASSP	SGI	YEQYF…
3A	…CASSP	AAA	YEQYF…

Figure 2.

The BEko.α- and β-chains and their CDR3 regions are required for binding the QFL ligand. (a) CD3 and GFP expression by C6VL.22(α ⁻) recipient cells transduced with BEko.α, C6VL.51(β ⁻) recipient cells transduced with BEko.β and 58 (α ⁻β ⁻) recipient cells transduced with both BEko.α- and BEko.β encoding retroviruses. (b) Fluorescent intensity of transduced cell lines expressing the BEko.α- or/and β chains stained with the QFL-tetramers labeled with phycoerythrin. (c) The amino acid sequence of the BEko.α- and β-chain CDR3 regions and the 4A and 3A alanine substitution mutants. (d) CD3 and GFP expression by the 58 (α ⁻β ⁻) cells transduced with both intact BEko.α- and β-chain, BEko.α pairing with BEko.β3A(3A) or BEko.β pairing with BEko.α4A(4A). (e) Fluorescent intensity of phycoerythrin labeled QFL-tetramer staining of the cell lines that express BEko.α- and β-chain (α+β), 4A paired with BEko.β-chain (4A+β) or 3A paired with BEko.α-chain (α+3A). Plots shown are representative of three independent experiments.

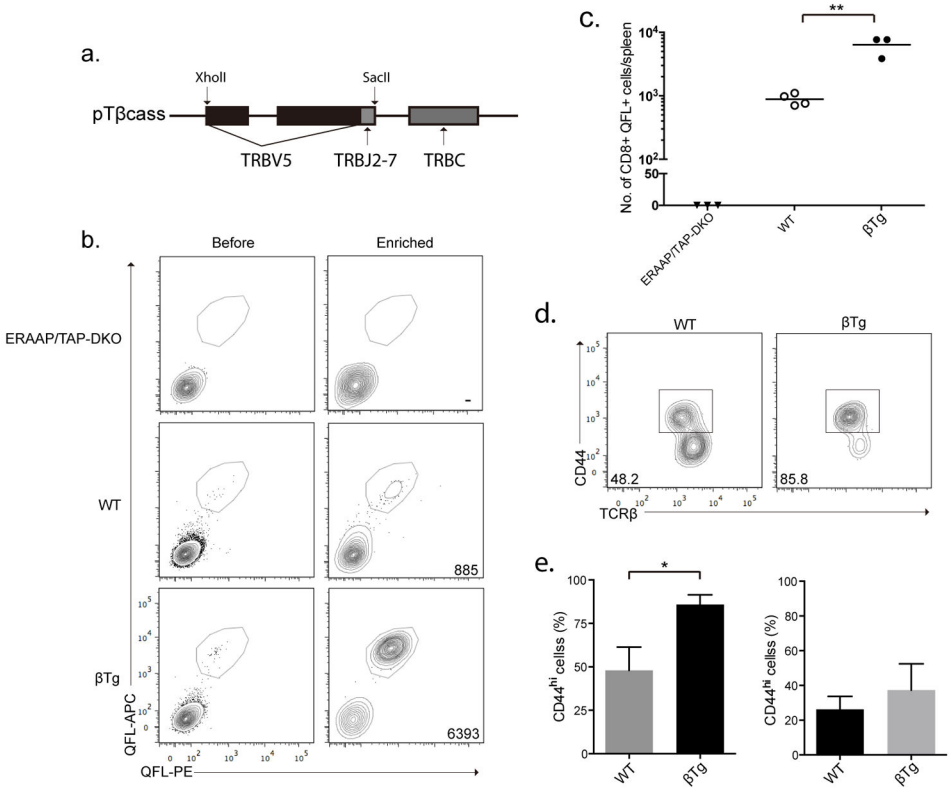

Figure 3.

Relative frequency of QFL-specific T cell in wild-type and BEko8Z TCR β-chain transgenic (βTg) mice. (a) Schematic representation of the rearranged TRBV5-TRBJ2-7 DNA cloned in the pTβcass vector for transgene expression. (b) Flow cytometry analysis of spleen cells from naïve ERAAP-TAP-DKO as negative control, wild-type and βTg mice, stained with QFL-tetramer labeled with phycoerythrin (QFL-PE) or allophycocyanin (QFL-APC) before (left) and after (right) enrichment of the tetramer$^+$ cells. Enrichment was carried out by positive selection of the magnetically labeled QFL-PE positive cells. Numbers in plots indicate the average number of QFL$^+$ T cells per spleen. (c) Numbers of QFL$^+$ T cells enriched per spleen in wild-type and βTg mice. Each symbol represents an individual animal. **= $p < 0.001$ (Student's T test). (d) Flow cytometry analysis of the enriched QFL$^+$ T cells from wild-type and βTg mice for CD44 expression. Numbers in plots indicate average percent of CD44^{hi}TCRβ$^+$ cells. (e) Frequency of CD44^{hi} cells among QFL$^+$ T cells and total CD8$^+$ T cells in wildtype and βTg mice. * = $p < 0.01$ (Student's T test). Results are shown as the mean ± SD of at least 3 mice (b,c) or 3 mice (d,e) per genotype and are representative of three independent experiments.

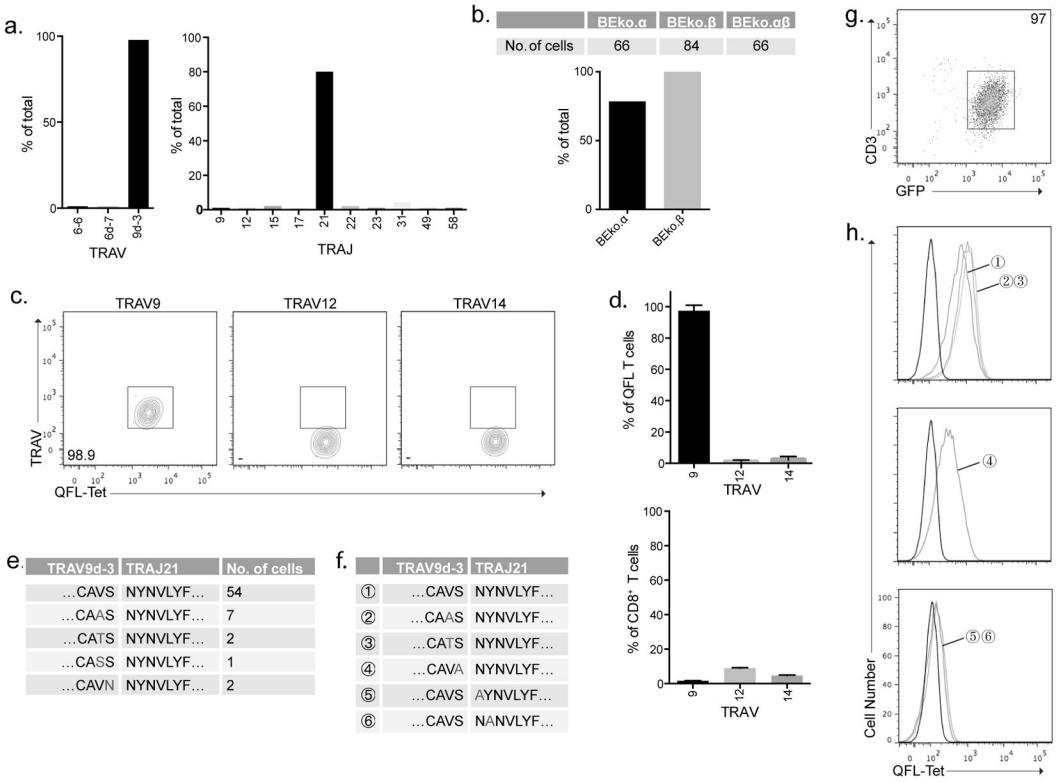

Figure 4.

The structure and function of the highly invariant TCR α chain expressed by QFL-specific T cells in naïve βTg spleen cells. (a) Frequency of Vα and Jα segments used by QFL-specific T cells was determined by single cell multiplex RT-PCR followed by sequencing 84 cells from 3 mice. (b) Numbers and frequency of the QFL-specific T cells that expressed BEko.α-, β-chain or both BEko. α- and β-chain in βTg mice. (c) Staining of the QFL-specific T cells with TRAV9, TRAV12 and TRAV14 specific antibodies. Numbers in the plots indicate percent of $TRAV^+$ cells detected. (d) Frequency of the $TRAV9^+$, $TRAV12^+$ and $TRAV14^+$ cells among QFL^+ or $CD8^+$ T cells from βTg mice. (e) The QFL-specific T cells bearing the wild-type or 4 natural variants within the CDR3 region of BEko.α-chain found in βTg mice. (f) Schematic representation of the wild-type (Ⓘ), natural variants (V>A or T) (②③) or artificial mutants (S/N/Y>A) (④-⑤) in CDR3 region of BEko.α-chain. (g) CD3 and GFP expression of the 58 ($\alpha^-\beta^-$) cells transduced with both intact BEko.α- and β-chain (Ⓘ) or BEko.β pairing with the BEko.α CDR3 region variants/mutants (②- ⑥). Plot is representative of the 6 αβ TCR transfectants. (h) QFL-tetramer fluorescence intensity of cell lines described in (f). Data is shown as mean ± SD and is representative of three experiments with three mice each.

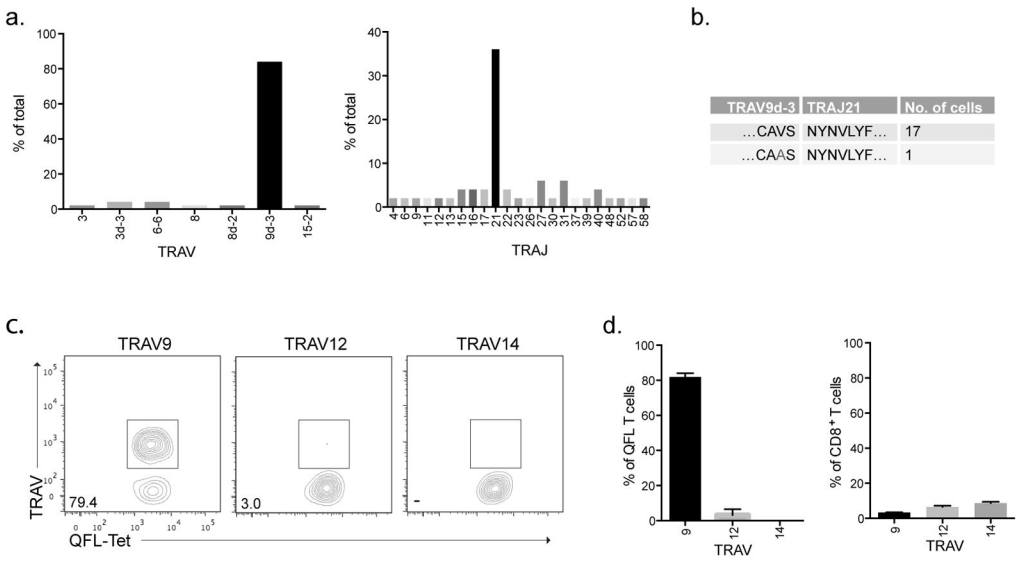

Figure 5.

The BEko.α-chain is expressed predominately by QFL-specific T cells enriched from naïve wild-type spleen cells. (a) Frequency of Vα and Jα segments used by 50 QFL-specific T cells in three wild-type mice. (b) Numbers of the QFL-specific T cells that used the wild-type or variant BEko.α-chain CDR3 region in wild-type mice. (c) Staining of the QFL T cells with TRAV9, TRAV12 and TRAV14 antibodies. Numbers in plot indicate percent of $TRAV^+$ cells. (d) Frequency of the $TRAV9^+$, $TRAV12^+$ and $TRAV14^+$ cells among QFL^+ or $CD8^+$ T cells. Data are representative of three experiments and shown as mean ± SD of nine mice.

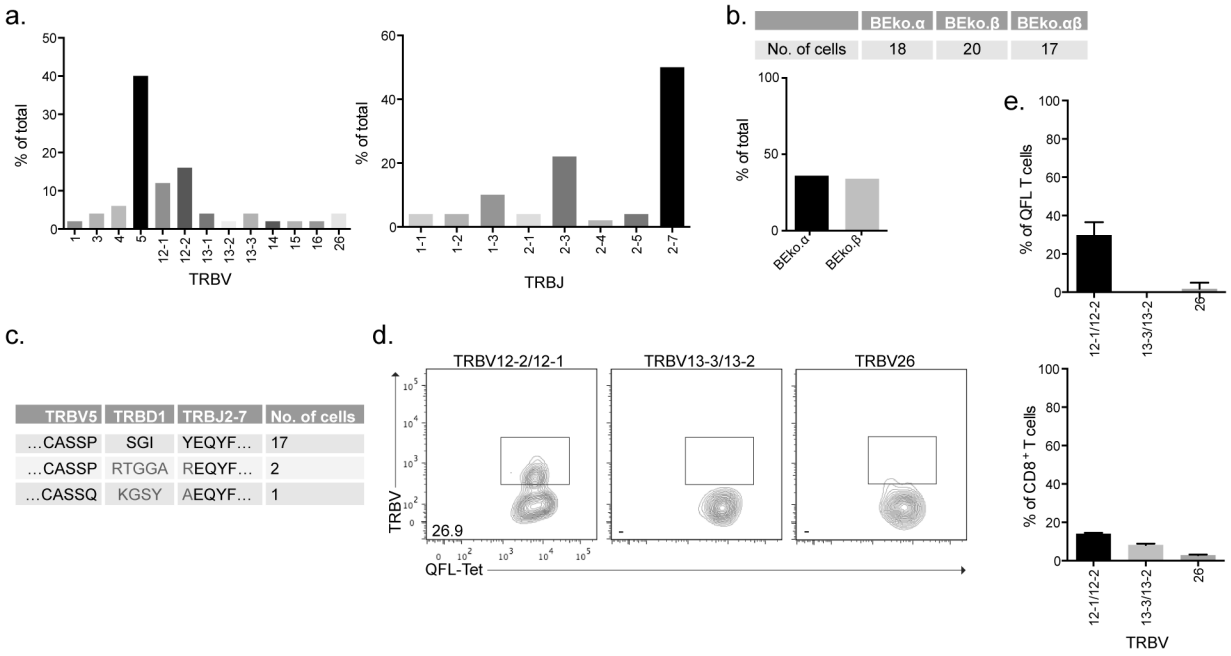

Figure 6.

The TCR β-chains used by QFL-specific T cells enriched from naïve wild-type spleen cells. (a) Frequency of the Vβ and Jβ segments used by the TCR β-chains pairing with the TCR α-chains analyzed above. (b) Numbers and frequency of QFL-specific T cells that expressed BEko.α-, β-chain or both the BEko.α- and β-chain in wild-type mice. (c) Number of QFL-specific T cells that express wild-type or variant BEko.β-chain CDR3 region in wild-type mice. (d) Staining of the QFL-specific T cells with TRBV12-2/12-1, TRBV13-3/13-2 and TRBV26 antibodies. Numbers in plot indicate percent of $TRBV^+$ cells. (e) Frequency of the $TRBV12\text{-}2/12\text{-}1^+$, $TRBV13\text{-}3/13\text{-}2^+$ or $TRBV26^+$ cells among QFL^+ or $CD8^+$ T cells. Data are representative of three experiments and shown as mean ± SD of nine mice.

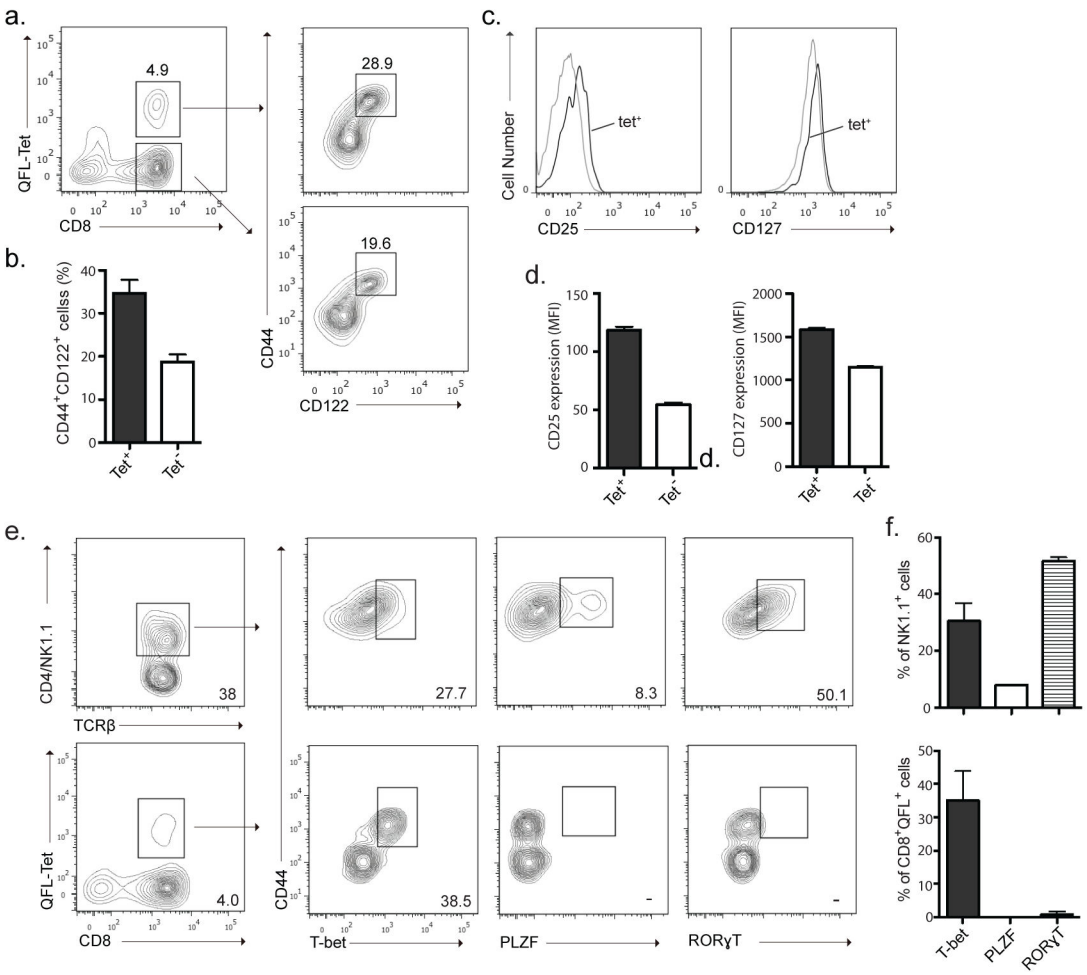

Figure 7.

Characterization of QFL-specific T cells in naïve wild-type B6 mice. (**a**) Flow cytometry of spleen cells, stained with QFL-PE tetramer and assessed after magnetic enrichment of the tetramer-positive cells. Numbers adjacent to the outlined area indicate percent $CD44^+CD122^+$ cells among $CD8^+QFL^+$ or the $CD8^+QFL^-$ cells. (**b**) Frequency of $CD44^+CD122^+$ cells among $CD8^+QFL^+$ cells or $CD8^+QFL^-$ cells after enrichment. (**c**) Fluorescence intensity of the QFL-Tet^+ or QFL-Tet^- cells stained with anti-CD25 or anti-CD127. (**d**) Mean Fluorescence Intensity (MFI) of CD25 or CD127 expression by QFL-Tet^+ or QFL-Tet^- cells. (**e**) Flow cytometry of transcription factors T-bet, PLZF or RORχT expression in the $CD44^{hi}$ $NK1.1^+$ or $CD8^+QFL^+$ cells. Numbers in the plots indicate average percent of T-bet^+, $PLZF^+$ or RORχT^+ cells. (**f**) Frequency of T-bet^+, $PLZF^+$ or RORχT^+ cells among the $CD44^{hi}$ $NK1.1^+$ or $CD8^+QFL^+$ cells. Data are representative of three experiments and shown as mean +/− s.e.m. of three mice.